Biostatistics (2011), **12**, 2, *pp.* 283–302
doi:10.1093/biostatistics/kxq059
Advance Access publication on September 14, 2010

C

Model structure analysis to estimate basic immunological processes and maternal risk for parvovirus B19

NELE GOEYVAERTS*

Interuniversity Institute for Biostatistics and Statistical Bioinformatics, Hasselt University, Agoralaan 1 Gebouw D, B3590 Diepenbeek, Belgium
nele.goeyvaerts@uhasselt.be

NIEL HENS

Interuniversity Institute for Biostatistics and Statistical Bioinformatics, Hasselt University, Agoralaan 1 Gebouw D, B3590 Diepenbeek, Belgium, and Centre for Health Economics Research and Modeling Infectious Diseases and Centre for the Evaluation of Vaccination, Vaccine & Infectious Disease Institute, University of Antwerp, Universiteitsplein 1, B2610 Wilrijk, Belgium

MARC AERTS

Interuniversity Institute for Biostatistics and statistical Bioinformatics, Hasselt University, Agoralaan 1 Gebouw D, B3590 Diepenbeek, Belgium

PHILIPPE BEUTELS

Centre for Health Economics Research and Modeling Infectious Diseases and Centre for the Evaluation of Vaccination, Vaccine & Infectious Disease Institute, University of Antwerp, Universiteitsplein 1, B2610 Wilrijk, Belgium

SUMMARY

After a steep monotone rise with age, the seroprevalence profiles for human parvovirus B19 (PVB19) display a decrease or plateau between the ages of 20 and 40, in each of 5 European countries. We investigate whether this phenomenon is induced by waning antibodies for PVB19 and, if this is the case, whether secondary infections are plausible, or whether boosting may occur. Several immunological scenarios are tested for PVB19 by fitting different compartmental dynamic transmission models to serological data using data on social contact patterns. The social contact approach has already been shown informative to estimate transmission rates and the basic reproduction number for infections transmitted predominantly through nonsexual social contacts. Our results show that for 4 countries, model selection criteria favor the scenarios allowing for waning immunity at an age-specific rate over the assumption of lifelong immunity, assuming that the transmission rates are directly proportional to the contact rates. Different views on the evolution of the immune response to PVB19 infection lead to altered estimates of the age-specific force of infection and the basic reproduction number. The scenarios which allow for multiple infections during one

*To whom correspondence should be addressed.

lifetime predict a higher frequency of PVB19 infection in pregnant women and of associated fetal deaths. When prevaccination serological data are available, the framework developed in this paper could prove worthwhile to investigate these different scenarios for other infections as well, such as cytomegalovirus.

Keywords: Age heterogeneity; Boosting; Bootstrap; Dynamic transmission model; Parvovirus B19; Risk in pregnancy; Seroepidemiology; Social contact pattern; Waning immunity.

1. INTRODUCTION

PVB19 was the first human parvovirus to be discovered in 1975, causing a range of diseases among which erythema infectiosum, commonly known as 5th disease of childhood or slapped cheek syndrome (Anderson and Cherry, 2004). In children and teenagers, the disease is usually mild, but in adults, especially women, it is often complicated by acute arthritis which may persist in some cases (Cohen, 1995). Infection with PVB19 during pregnancy has been associated with intrauterine fetal death, fetal anemia, and hydrops fetalis (Tolfvenstam *and others*, 2001). From the onset of rash or arthralgia, the infected individual is usually no longer contagious, which complicates the detection and control of the virus. Furthermore, subclinical PVB19 infection is a common finding in both children and adults (Heegaard and Brown, 2002). Although it is under development, there is currently no vaccine available for PVB19.

After being infected with PVB19, individuals acquire immunoglobulin G (IgG) antibodies against PVB19, and it is generally assumed that these antibodies persist for a lifetime (Young and Brown, 2004). Since the presence of IgG antibodies indicates past infection with PVB19 and the duration of exposure to infection increases with age, the proportion of seropositives should be monotone increasing with age, provided that there is time equilibrium at the disease (endemic) and population level (demographic), and that mortality attributable to PVB19 infection can be ignored. However, after an initial monotone increase with age, the seroprevalence profiles for PVB19 from 5 European countries show a decrease or plateau between the ages of 20 and 40, after which the prevalence continues to monotonically increase with age (Figure 2). This phenomenon does not support the assumption of lifelong immunity. Given the evidence from the literature summarized in Appendix A of the Supplementary Material available at *Biostatistics* online (e.g. Nascimento *and others*, 1990), a cohort effect due to an epidemic or a demographical shift seems very unlikely.

Hypotheses of waning of IgG antibodies, boosting by exposure to infectious individuals and reinfections, were suggested before (Schoub *and others*, 1993; Kaufmann *and others*, 2007; Vyse *and others*, 2007; Huatuco *and others*, 2008; Schneider *and others*, 2008), however up till now these hypotheses have never been tested using empirical data. Gay (1996) used a mixture modeling approach to describe the distribution of continuous PVB19 IgG antibody titers and noted a significant increase with age in the left skewness of the seropositive population, particularly after 20 years of age, suggesting a decay of antibody levels. Gaining insight in the processes underlying PVB19 transmission dynamics is of major public health interest since the decrease or plateau in IgG seroprevalence is specifically observed in women of child-bearing age.

In the absence of longitudinal antibody titer data for PVB19 which would enable us to study the evolution of IgG antibodies directly, we propose an alternative approach. We explore several immunological scenarios in mathematical models and infer on waning and boosting rates using serological and social contact data (Goeyvaerts *and others*, 2010), assessing whether the scenarios are able to explain the observed decrease in the seroprevalence profile for adults. Similar models were considered before for measles (Rouderfer *and others*, 1994) and pertussis (van Boven *and others*, 2000, 2001). However in these studies, values for waning and boosting rates were predefined and, in the absence of representative social contact surveys, proportionate mixing was assumed. Inference on transmission dynamics of PVB19 is

important for diagnosis, assessing the risk of prenatal infection and designing future vaccination policies. If a significant proportion of the population is infected twice or more with PVB19, it is likely that many secondary infections are asymptomatic or atypical and hence may not be noticed by traditional surveillance systems based on case reporting. The risk in pregnant women is then likely underestimated and a larger proportion of undiagnosed fetal complications may therefore be attributable to PVB19 infection during pregnancy.

The paper is organized as follows. In Section 2, we describe the different data sources informing our model structure analysis for PVB19 in 5 European countries: seroprevalence profiles, demographic data, and social contact surveys. The compartmental transmission scenarios we consider for PVB19 are introduced in Section 3.1. We divide the mathematical scenarios into 3 types of dynamics; the first type discerning between high and low "waned" immunity (Maternally derived immunity-Susceptible-Infectious-Recovered (high immunity)-Waned (low immunity) [MSIRW]), the second type allowing for multiple infections (Maternally derived immunity-Susceptible-Infectious-Recovered (immunity)-Susceptible [MSIRS]) and the third type being a mixture of the 2 previous ones (MSIRWS). For each scenario, exact formulas for the age-specific proportions of susceptible and seropositive individuals are derived. These are incorporated into the maximum likelihood (ML) procedure to estimate the unknown parameters on PVB19 transmission, immunology, and risk in pregnancy, which is described further on in Section 3.2. In Section 4, we present the results of this model structure analysis and summarize the main findings using different inferential means. Some final conclusions and a discussion are given in Section 5.

2. Data

In Belgium (BE), England and Wales (EW), Finland (FI), Italy (IT), and Poland (PL), a seroprevalence survey was conducted totaling 13 449 serum samples collected between 1995 and 2004 (Mossong, Hens, Friederichs, *and others*, 2008). The serum samples were tested for the presence of IgG antibodies against PVB19, and the same batch of a commercial immunoassay test was used for each country (Mikrogen recomWell, Martinsried, Germany). The few equivocal results, located within the cutoff range specified by the manufacturer, are spread over all age groups and excluded from the analysis. The univocal serological data, of which a short summary is presented in Appendix B of the Supplementary Material available at *Biostatistics* online, were analyzed before using monotone local polynomials (Mossong, Hens, Friederichs, *and others*, 2008).

We use truncated poststratification weights $\tilde{w}_i$ to make the serological data representative of the different populations (cf. Appendix B of the Supplementary Material available at *Biostatistics* online). Further, our modeling approach to PVB19 transmission assumes a large population of fixed size N and demographic equilibrium with $N(a)$ the stationary age distribution for the population size and $\mu(a)$ the age-specific mortality rate. To estimate the frequency and burden of PVB19 infection during pregnancy, we need the maternal age distribution for live births, denoted by $B(a)$. Country-specific estimates of these figures are obtained from demographic data as described in Appendix B of the Supplementary Material available at *Biostatistics* online.

Comparable to rubella, PVB19 is primarily spread from person to person by infected respiratory droplets, and thus mathematical models of PVB19 transmission will require assumptions on age-related mixing patterns. In Appendix B of the Supplementary Material available at *Biostatistics* online, we provide a brief account of PVB19 outbreak reports and risk groups in a social context. Since 1997, several small scale surveys were made in order to gain more insight in social mixing behavior relevant to the spread of close contact infections (see, e.g. Edmunds *and others*, 1997). To refine on contact information, a large multicountry population–based survey was conducted in Europe between May, 2005 and September, 2006, as part of the Improving public health policy in Europe through modelling and economic evaluation of interventions for the control of infectious diseases (POLYMOD) project. For an extensive description

of the contact survey together with some exploratory data analysis, we refer to Mossong, Hens, Jit, *and others* (2008). In this paper, we use contact data from the 5 countries under study for PVB19: BE, Great Britain (GB) (which encompasses EW), FI, IT, and PL. A short summary of the data is provided in Appendix B of the Supplementary Material available at *Biostatistics* online.

3. TRANSMISSION SCENARIOS FOR PVB19

3.1 *Mathematical models*

We will consider several compartmental scenarios to model the dynamics of PVB19 transmission. In general, compartmental models represent age- and time-dependent dynamical models describing the flow of individuals through different mutually exclusive infection states. The basic building block will be an MSIR structure assuming that newborns are protected by maternal antibodies (first stage, denoted "M") until waning results in loss of passive immunity, and the infants become susceptible to infection (second stage, denoted "S"). As they age from then on, they may become infected and infectious to others (third stage, denoted "I"). After infection, they recover and acquire immunity, which is expressed through their IgG antibody level (fourth stage, denoted "R"). The corresponding number of individuals in each stage or compartment can be expressed as a function of age and time by $M(a,t)$, $S(a,t)$, $I(a,t)$, and $R(a,t)$, respectively.

In this paper, we will assume endemic equilibrium, which means that at the population level the infection is in an endemic steady state. In the following, lowercase letters indicate age-specific proportions by compartment, for example, $s(a) = S(a)/N(a)$, where $N(a)$ is the age-specific population size. Further, we assume type I maternal antibodies, $m(a) = 1$ if $a \leqslant A$ and $m(a) = 0$ if $a > A$, where A is the age at which maternal antibodies are lost, and ignore mortality due to infection which is justified for PVB19. If the mean duration of infectiousness D is short compared to the timescale on which transmission and mortality rates vary, the force of infection $\lambda(a)$ can be approximated by (e.g. Anderson and May, 1991)

$$\lambda(a) = D\int_A^\infty \beta(a,a')\lambda(a')S(a')\mathrm{d}a', \tag{3.1}$$

where $\beta(a,a')$ denotes the transmission rate, that is, the *per capita* rate at which an individual of age a' makes an effective contact with a person of age a, per year. Formula (3.1) reflects the so-called "mass action principle," which implicitly assumes that infectious and susceptible individuals mix completely with each other and move randomly within the population.

To investigate the assumption of lifelong immunity, we fit the basic MSIR model to the serological data and compare its fit to specific mathematical scenarios described hereunder, comprising processes of waning, boosting, and reinfection with PVB19.

MSIRW models. Figure 1(a) shows a graphical representation of the "MSIRWb-ext" model, which allows for waning of disease-acquired antibodies without loss of protective ("cellular") immunity. Individuals then move at a rate $\varepsilon(a)$ from a high immunity state R to a low immunity state W in which they are still protected from infection however categorized as being seronegative, that is, with antibody levels (indicating "humoral" immunity) falling below the serostatus threshold. We assume that low immunity can be boosted by exposure to infectious individuals. The boosting rate and the force of infection are then directly proportional with a proportionality constant φ, such that the rate at which individuals move back from W to R equals $\varphi \cdot \lambda(a)$. By solving the corresponding set of differential equations, one finds that the fraction in state S equals

$$s(a) = \exp\left(-\int_A^a \lambda(u)\mathrm{d}u\right) \quad \text{if } a > A. \tag{3.2}$$

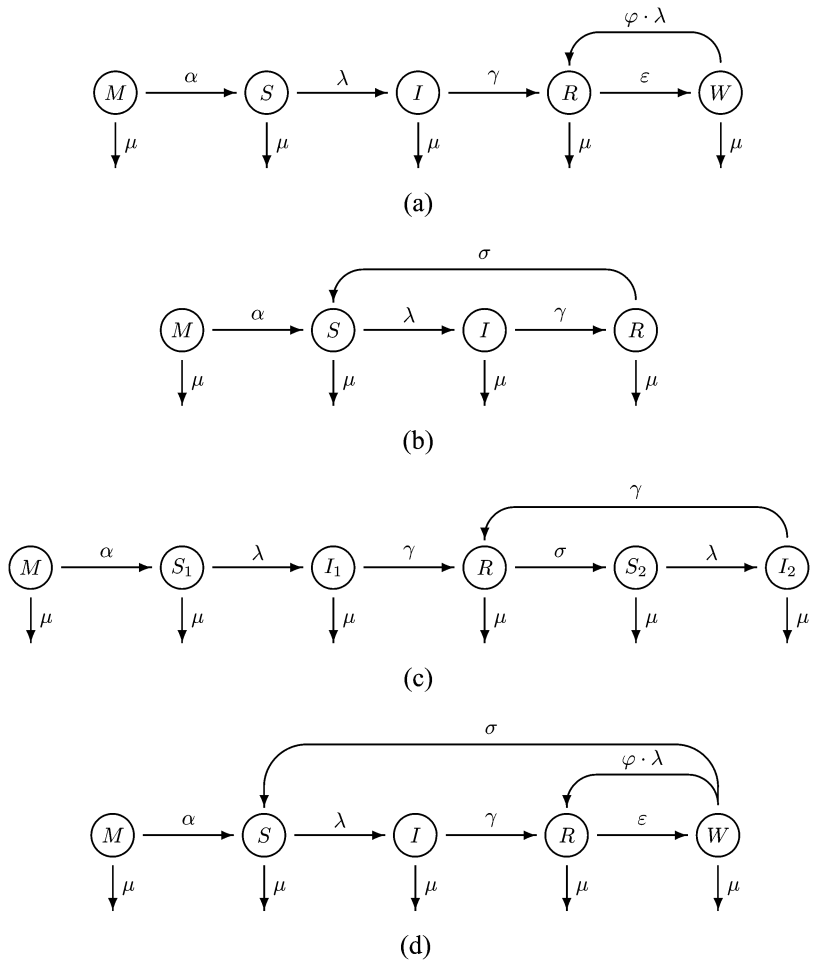

Fig. 1. Illustration of the MSIRWb-ext (a), MSIRS (b), MSIRS-ext (c), and MSIRWS (d) compartmental models.

Approximating $r(a)$ by $1 - s(a) - w(a)$, $\forall\, a > A$, assuming $i(a)$ is small relative to $s(a)$ and $w(a)$, we obtain the following expression for the proportion seropositives:

$$r(a) = \int_A^a \left\{ (1-\varphi)\lambda(u) \exp\left(-\int_A^u \lambda(v)\mathrm{dv} \right) + \varphi\lambda(u) \right\} \exp\left(-\int_u^a \{\varphi\lambda(v) + \varepsilon(v)\}\mathrm{dv} \right) \mathrm{du},$$

if $a > A$. The 2 special cases in which there is no boosting of low immunity, $\varphi = 0$, and in which the boosting rate exactly equals the force of infection, $\varphi = 1$, as assumed by Rouderfer *and others* (1994), are considered as well and denoted by "MSIRW" and "MSIRWb," respectively.

MSIRS models. The MSIRS model, displayed in Figure 1(b), allows for loss of disease-acquired immunity and potential reinfection. Individuals are assumed to move from R back to the susceptible state S at a rate $\sigma(a)$. Again, by solving the corresponding set of differential equations and making use of $r(a) \approx 1 - s(a)$, $\forall\, a > A$, expressions for the proportion of susceptibles and seropositives can be

obtained:

$$s(a) = \exp\left(-\int_A^a \{\lambda(u) + \sigma(u)\}\,\mathrm{du}\right) + \int_A^a \sigma(u)\exp\left(-\int_u^a \{\lambda(v) + \sigma(v)\}\mathrm{dv}\right)\mathrm{du} \quad \text{if a} > \text{A},$$

$$r(a) = \int_A^a \lambda(u)\exp\left(-\int_u^a \{\lambda(v) + \sigma(v)\}\mathrm{dv}\right)\mathrm{du} \quad \text{if a} > \text{A}. \tag{3.3}$$

The $\mathrm{MS_1I_1RS_2I_2RS_2}$ model (denoted "MSIRS-ext"), presented in Figure 1(c), is an extension of the MSIRS model and closely follows the model of van Boven *and others* (2000, 2001) for pertussis. This scenario allows to distinguish between infection in immunologically naive individuals (I_1) and infection in individuals whose immune system has been primed by infection before (I_2). The proportion of immunologically naive susceptibles $s_1(a)$ is given by (3.2), and the set of differential equations yields the following solutions, assuming γ is large and thus $r(a) \approx 1 - s_1(a) - s_2(a)$:

$$s_2(a) = \int_A^a \sigma(u)\left\{1 - \exp\left(-\int_A^u \lambda(v)\mathrm{dv}\right)\right\}\exp\left(-\int_u^a \{\sigma(v) + \lambda(v)\}\mathrm{dv}\right)\mathrm{du},$$

if $a > A$, and the fraction of seropositives is given by formula (3.3). In the MSIRS-ext framework, the mass action principle (3.1) is rewritten as

$$\lambda(a) = D\int_A^\infty \{\beta_1(a,a')\lambda(a')S_1(a') + \beta_2(a,a')\lambda(a')S_2(a')\}\mathrm{da}', \tag{3.4}$$

where $\beta_1(a,a')$ and $\beta_2(a,a')$ are the group-specific age-dependent transmission rates.

MSIRWS model. The MSIRWS model (Figure 1(d)) is an adaptation of the model by Rouderfer *and others* (1994) for measles, and can be seen as a mixture of the MSIRWb-ext model and the MSIRS model. Individuals in the low immunity state W can either be boosted by exposure to infectious individuals and move back to the high immunity state R at a rate $\varphi \cdot \lambda(a)$, or their immunity wanes to such an extent that they become susceptible again at a rate $\sigma(a)$. Approximating $r(a)$ by $1 - s(a) - w(a)$, assuming $i(a)$ is small, we obtain the following system of differential equations for $s(a)$ and $w(a)$:

$$\begin{cases} s'(a) &= \sigma(a)w(a) - \lambda(a)s(a), \\ w'(a) &= \varepsilon(a)\{1 - s(a)\} - \{\varphi\lambda(a) + \sigma(a) + \varepsilon(a)\}w(a). \end{cases}$$

This system of inhomogeneous linear differential equations of order 1 and dimension 2 cannot be solved explicitly for $s(a)$ and $w(a)$. However, by turning to discrete age classes, the solutions can be approximated recursively (cf. Appendix C of the Supplementary Material available at *Biostatistics* online).

3.2 *Inference on PVB19 immunology and risk in pregnancy*

First, we assume that the transmission rates $\beta(a,a')$ (3.1) are directly proportional to age-specific rates of making social contact, $c(a,a')$, with a disease-specific proportionality factor q (Wallinga *and others*, 2006): $\beta(a,a') = q \cdot c(a,a')$, referred to as the "constant proportionality assumption." The contact rates are estimated from the POLYMOD contact survey using a nonparametric model as described in Appendix D of the Supplementary Material available at *Biostatistics* online. Since the integral equation (3.1) has no closed-form solution, we then turn to discrete age classes to estimate the scenario-specific parameters $\boldsymbol{\varepsilon}$, $\boldsymbol{\sigma}$, φ, and $\boldsymbol{q}$ (cf. Appendix C of the Supplementary Material available at *Biostatistics*

online). Through an iterative procedure, the Bernoulli log-likelihood for the serological data is maximized (cf. "Matlab" code in Appendix G of the Supplementary Material available at *Biostatistics* online):

$$\ell(\boldsymbol{\varepsilon}, \boldsymbol{\sigma}, \varphi, \boldsymbol{q}|y_1, \ldots, y_n) = \sum_{i=1}^{n} \tilde{\omega}_i \{y_i \log[r(a_i|\boldsymbol{\varepsilon}, \boldsymbol{\sigma}, \varphi, \boldsymbol{q})] + (1 - y_i) \log[1 - r(a_i|\boldsymbol{\varepsilon}, \boldsymbol{\sigma}, \varphi, \boldsymbol{q})]\},$$

where n denotes the sample size of the serological data set, y_i the binary variable indicating whether subject i of age a_i is classified as being seropositive, and $\tilde{\omega}_i$ the individual's poststratification weight (Section 2).

Once the ML estimates of these parameters are obtained, the basic reproduction number R_0, that is, the number of secondary cases produced by a typical infected person during his or her entire period of infectiousness when introduced into an entirely susceptible population, is calculated as the dominant eigenvalue of the next generation matrix with elements $D\big(\int_{a_{[i]}}^{a_{[i+1]}} N(a)\,\mathrm{da}\big)\beta_{\mathrm{ij}}$ (Diekmann *and others*, 1990). In the first application, we assume that the proportionality factor q and the immunity transition rates ε and σ are independent of age. Next, the latter assumption is relaxed by modeling the waning rate as a piecewise constant function with a cutoff point at a predetermined age H: $\varepsilon(a) = \varepsilon_1$, if $a \in (A, H)$, and $\varepsilon(a) = \varepsilon_2$, if $a \geqslant H$, and similar for $\sigma(a)$. This model is able to identify age differences in the rate at which antibody levels decay. As in Goeyvaerts *and others* (2010), we assess the sensitivity of our results with respect to the constant proportionality assumption by generalizing to "age-dependent proportionality": $\beta(a, a') = q(a, a') \cdot c(a, a')$. Discrete matrix structures are considered to model $q(a, a')$ (cf. Appendix D of the Supplementary Material available at *Biostatistics* online).

Risk in pregnancy. To assess the infection risk in pregnant women, we estimate the average maternal proportion of susceptibles ($\bar{s}_{\mathrm{p}}$) and the average maternal force of infection ($\bar{\lambda}_{\mathrm{p}}$),

$$\bar{s}_{\mathrm{p}} = \frac{\int_0^\infty s(a)B(a)\,\mathrm{da}}{\int_0^\infty B(a)\,\mathrm{da}}, \quad \bar{\lambda}_{\mathrm{p}} = \frac{\int_0^\infty \lambda(a)s(a)B(a)\,\mathrm{da}}{\int_0^\infty s(a)B(a)\,\mathrm{da}},$$

where $B(a)$ represents the maternal age distribution of live births as introduced in Section 2. The annual number of PVB19 infections in pregnant women is calculated as follows (Gay *and others*, 1994): $I_{\mathrm{p}} = 0.77 \int_0^\infty \lambda(a)s(a)B(a)\,\mathrm{da}$, where 0.77 embodies the mean duration of pregnancy (40 weeks). To estimate the frequency of fetal deaths due to PVB19 infection during pregnancy, we calculate an average risk of fetal loss using data from the 2 largest prospective cohort studies of pregnant women with confirmed PVB19 infection reported in the literature: a study from EW (1985–1988 and 1992–1995) by Miller *and others* (1998) and from Germany (1993–1998) by Enders *and others* (2004). We find an average excess fetal death rate during the first 20 weeks of gestation of 7.7%, when comparing the study populations to a control group of women in EW and Germany who were followed up prospectively after varicella infection in pregnancy (Enders *and others*, 1994). Pastuszak *and others* (1994) showed that there is no significant difference in the rate of fetal loss between women with and women without primary varicella infection during pregnancy. Although Tolfvenstam *and others* (2001) suggest that fetal death due to PVB19 infection in late second and third trimester of pregnancy could be more common than previously reported, a recent study by Riipinen *and others* (2008) confirms the results of Miller *and others* (1998) and Enders *and others* (2004) that this is overall a very rare event.

Table 1. *ML estimates for the scenario-specific parameters $q, \varepsilon, \sigma, \varphi$, and the basic reproduction number R_0, with 95% bootstrap-based percentile CIs in square brackets, information criteria AIC and BIC (minima indicated in boldface), and LR test null hypotheses and p-values, obtained under the assumption of CW*

Country	Model				$\hat{R}_0$		AIC	BIC	LR test	
									H_0	p-value
BE	MSIR	$\hat{q}$	0.056	[0.047, 0.062]	2.48	[2.27, 2.72]	3477.08	3483.10		
	MSIRW	$\hat{q}$	0.073	[0.058, 0.087]	3.21	[2.70, 3.93]	3390.20	3402.26		
		$\hat{\varepsilon}$	0.004	[0.002, 0.006]					$\varepsilon = 0$	<0.001
	MSIRWb	$\hat{q}$	0.076	[0.060, 0.093]	3.35	[2.77, 4.17]	**3384.02**	**3396.07**		
		$\hat{\varepsilon}$	0.010	[0.005, 0.014]					$\varepsilon = 0$	<0.001
	MSIRWb-ext	$\hat{q}$	0.076	[0.059, 0.093]	3.35	[2.77, 4.17]	3385.98	3404.06		
		$\hat{\varepsilon}$	0.009	[0.005, 0.021]					$\varphi = 0$	0.006
		$\hat{\varphi}$	0.91	[0.30, 2.56]					$\varphi = 1$	0.841
	MSIRS	$\hat{q}$	0.064	[0.054, 0.072]	2.84	[2.54, 3.22]	3387.51	3399.56		
		$\hat{\sigma}$	0.013	[0.006, 0.022]					$\sigma = 0$	<0.001
	MSIRS-ext	$\hat{q}_1$	0.076	[0.000, 0.091]	3.35	[0.00, 4.10]	3386.02	3404.10		
		$\hat{q}_2$	0.000	[0.000, 0.132]					$q_1 = q_2$	0.062
		$\hat{\sigma}$	0.010	[0.005, 0.044]						
EW	MSIR	$\hat{q}$	0.053	[0.047, 0.057]	1.72	[1.64, 1.81]	3551.25	3557.20		
	MSIRW	$\hat{q}$	0.058	[0.050, 0.064]	1.87	[1.72, 2.04]	3533.53	3545.42		
		$\hat{\varepsilon}$	0.003	[0.000, 0.005]					$\varepsilon = 0$	<0.001
	MSIRWb	$\hat{q}$	0.059	[0.051, 0.065]	1.90	[1.73, 2.07]	**3531.65**	**3543.54**		
		$\hat{\varepsilon}$	0.004	[0.001, 0.008]					$\varepsilon = 0$	<0.001
	MSIRWb-ext	$\hat{q}$	0.059	[0.051, 0.065]	1.91	[1.74, 2.09]	3532.21	3550.05		
		$\hat{\varepsilon}$	0.008	[0.002, 0.025]					$\varphi = 0$	0.034
		$\hat{\varphi}$	3.16	[0.94, 12.5]					$\varphi = 1$	0.230
	MSIRS	$\hat{q}$	0.057	[0.050, 0.061]	1.83	[1.71, 1.96]	3531.88	3543.77		
		$\hat{\sigma}$	0.005	[0.001, 0.008]					$\sigma = 0$	<0.001
	MSIRS-ext	$\hat{q}_1$	0.059	[0.026, 0.064]	1.90	[0.89, 2.06]	3533.65	3551.49		
		$\hat{q}_2$	0.000	[0.000, 0.364]					$q_1 = q_2$	0.632
		$\hat{\sigma}$	0.004	[0.001, 0.011]						
FI	MSIR	$\hat{q}$	0.052	[0.045, 0.057]	1.56	[1.52, 1.64]	**3055.50**	**3061.32**		
	MSIRW	$\hat{q}$	0.052	[0.045, 0.057]	1.56	[1.52, 1.65]	3057.50	3069.15		
		$\hat{\varepsilon}$	0.000	[0.000, 0.001]					$\varepsilon = 0$	1.000
	MSIRWb	$\hat{q}$	0.052	[0.045, 0.057]	1.56	[1.52, 1.65]	3057.50	3069.15		
		$\hat{\varepsilon}$	0.000	[0.000, 0.002]					$\varepsilon = 0$	1.000
	MSIRS	$\hat{q}$	0.052	[0.045, 0.057]	1.56	[1.52, 1.65]	3057.50	3069.15		
		$\hat{\sigma}$	0.000	[0.000, 0.002]					$\sigma = 0$	1.000

Continued on next page

Table 1. *Continued*

Country	Model				$\hat{R}_0$		AIC	BIC	LR-test	
									H_0	p-value
IT	MSIR	$\hat{q}$	0.025	[0.021, 0.027]	1.68	[1.60, 1.79]	3192.52	3198.35		
	MSIRW	$\hat{q}$	0.027	[0.023, 0.030]	1.86	[1.68, 2.04]	3176.16	3187.82		
		$\hat{\varepsilon}$	0.003	[0.000, 0.005]					$\varepsilon = 0$	<0.001
	MSIRWb	$\hat{q}$	0.028	[0.023, 0.030]	1.89	[1.69, 2.08]	**3175.12**	**3186.78**		
		$\hat{\varepsilon}$	0.004	[0.001, 0.007]					$\varepsilon = 0$	<0.001
	MSIRS	$\hat{q}$	0.027	[0.023, 0.029]	1.83	[1.68, 1.99]	3175.96	3187.62		
		$\hat{\sigma}$	0.005	[0.001, 0.008]					$\sigma = 0$	<0.001
	MSIRS-ext	$\hat{q}_1$	0.028	[0.022, 0.030]	1.89	[1.58, 2.08]	3177.12	3194.61		
		$\hat{q}_2$	0.000	[0.000, 0.118]					$q_1 = q_2$	0.359
		$\hat{\sigma}$	0.004	[0.001, 0.008]						
PL	MSIR	$\hat{q}$	0.047	[0.041, 0.050]	2.16	[1.97, 2.31]	**2785.69**	**2791.51**		
	MSIRW	$\hat{q}$	0.047	[0.041, 0.051]	2.16	[1.97, 2.32]	2787.69	2799.33		
		$\hat{\varepsilon}$	0.000	[0.000, 0.000]					$\varepsilon = 0$	1.000
	MSIRWb	$\hat{q}$	0.047	[0.041, 0.051]	2.16	[1.97, 2.32]	2787.69	2799.33		
		$\hat{\varepsilon}$	0.000	[0.000, 0.001]					$\varepsilon = 0$	1.000
	MSIRS	$\hat{q}$	0.047	[0.041, 0.050]	2.16	[1.97, 2.31]	2787.69	2799.33		
		$\hat{\sigma}$	0.000	[0.000, 0.001]					$\sigma = 0$	1.000

4. Results

4.1 *Constant waning*

For the remainder of the paper, we assume that the mean duration of infectiousness for PVB19 is $D = 6/365$ years (Anderson and Cherry, 2004) and that maternally derived antibodies are lost at the age of $A = 0.5$ years, implying that neonates younger than 6 months are assumed not to take part in the PVB19 transmission process (see, e.g. Huatuco *and others*, 2008). The few serological samples of neonates younger than 6 months, which are only covered by the sample for BE, are therefore removed. Further, we consider integer age intervals for all countries: $(0.5, 1), [1, 2), [2, 3), \ldots, [79, 80)$. The different dynamical models are fitted to the serological data, assuming constant waning (CW) rates ε and σ, and constant proportionality with respect to close contacts >15 min. Confidence intervals (CIs) are obtained using the nonparametric bootstrap approach described in Goeyvaerts *and others* (2010), taking into account all sources of sampling variability and age uncertainty. The ML estimates for the scenario-specific parameters and R_0 are displayed in Table 1, together with 95% bootstrap-based percentile CIs and information criteria Akaikes Information Criterion (AIC) and Bayesian Information Criterion (BIC). Figure 2 depicts the estimated seroprevalence and force of infection for the MSIR model and the best model according to AIC/BIC.

Likelihood ratio (LR) tests are performed to test the null hypotheses $H_0: \varepsilon = 0$ and $H_0 : \sigma = 0$ for the MSIRW and MSIRS models, respectively. Since these null hypotheses are on the boundary of the parameter space $\mathbb{R}^+$, the asymptotic distribution of the LR test statistic is a 50:50 mixture of χ^2_0 and χ^2_1 (Self and Liang, 1987). The p-values together with the information criteria in Table 1 indicate substantial evidence against the assumption of lifelong immunity for PVB19 in BE, EW, and IT. Note that, except

for MSIRW in IT, the same conclusion can be made from the 95% CIs for ε and σ, which also take into account the variability originating from the contact data. For these countries, the MSIRW scenario with boosting comes out as the "best" model and is therefore displayed in Figure 2. AIC and BIC values for MSIRW and MSIRS models are, however, fairly close and the estimated seroprevalence profiles are nearly indistinguishable (suppressed from Figure 2). For FI and PL, however, the scenarios are not able to elicit any evidence of waning immunity from the PVB19 serology, and the fit is identical to the MSIR case (see Table 1 and Figure 2).

The results from MSIRWb-ext and MSIRS-ext for both FI and PL are omitted from Table 1 since ε and σ are estimated to be zero, making neither $\hat{\varphi}$ nor $\hat{q}_2$ estimable. The results from MSIRWb-ext are omitted for IT as well since 90% of the bootstrap replicates of $\hat{\varepsilon}$ are larger than 10^3. The unboundedness of the parameters and the structure of the Italian serological data conduce to extremely large bootstrap estimates for both ε and φ, which is unrealistic and noninterpretable. For BE and EW, we additionally test whether the proportionality constant φ in the MSIRWb-ext model equals 0 or 1, corresponding to MSIRW and MSIRWb, respectively. The former null hypothesis is on the boundary of the parameter space $\mathbb{R}^+$, while the latter hypothesis of $H_0: \varphi = 1$ implies a classical LR test. For BE and EW, there is a significant amount of boosting and the boosting rate is not significantly different from the force of infection.

To test the need of extending the MSIRS model, an LR test of $H_0: q_1 = q_2$ is performed for MSIRS-ext. The nonsignificant p-values together with AIC and BIC values demonstrate the limited impact on the fit to the data. Further, the bootstrap samples mainly give rise to 2 discrepant solutions: $\hat{q}_1 = 0$ or $\hat{q}_2 = 0$. We believe we cannot identify differences in transmission potential with respect to the immunological status of the infected individual because the serological data only provide information related to susceptibility. Therefore, MSIRS-ext is not considered further when relaxing the CW assumption. Note that in the latter framework, we have calculated the basic reproduction number based on a typical "primary" infected person, such that bootstrap replicates $\hat{q}_1 = 0$ correspond to $\hat{R}_0 = 0$, clarifying the lower CI limits for BE and EW.

Solutions for the MSIRWS model are obtained using numerical approximation, however, these results are not presented here since they are not directly comparable with those for the other models in Table 1, which are obtained from analytical solutions. Nevertheless, for BE and EW, we are able to compare the fit of MSIRWS with MSIRWb-ext and MSIRS by constraining the parameters to the following values: $\sigma = 0$ and $(\varphi, \sigma) = (0, 200)$, respectively. The MSIRWS model is not better according to the BIC criterion and therefore omitted from further consideration.

Considering the best models in terms of AIC/BIC, the following estimates are obtained for the basic reproduction number R_0: 3.35 for BE, 1.90 for EW, 1.56 for FI, 1.89 for IT, and 2.16 for PL. The estimated basic reproduction number for PVB19 is similar for EW, IT and PL. R_0 is significantly smaller for Finland and significantly larger for Belgium compared to the other countries, which may indicate an epidemiological difference. A visual inspection of the fit to the data (Figure 2) reveals that for BE, EW, and PL, the CW scenarios are not able to capture the decrease or plateau observed in the seroprofile for young adults. Therefore, in the next section, we further generalize these scenarios and relax the assumption that the waning rates are independent of age.

4.2 *Age-specific waning*

We extend the CW models from the previous section to allow for age differences in the immunity transition rates ε and σ. Ten piecewise constant functions are fitted to the data with cutoff points H ranging from 5 to 50 years in 5 years steps. For FI, allowing for age-related heterogeneity in the rate at which antibody levels wane over time, has virtually no effect on the fit to the seroprevalence data and the resulting parameter estimates. For BE, EW, and PL, there is a large improvement in fit, and the likelihood values for the 4 scenarios as functions of H clearly show maxima between the ages 20 and 50. For IT, the impact on the

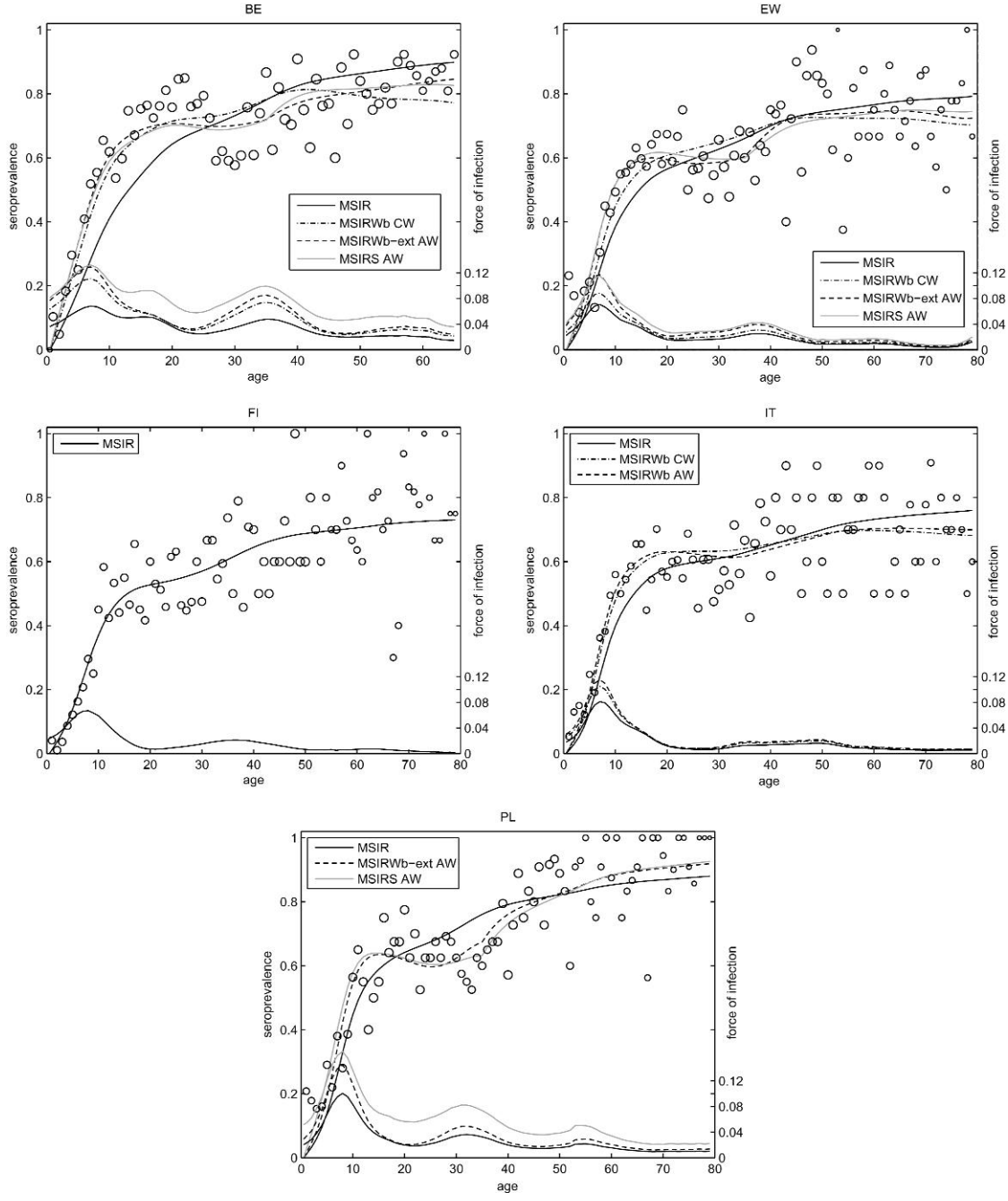

Fig. 2. Estimated seroprevalence (upper curves) and corresponding force of infection (lower curves) obtained for a number of selected transmission scenarios for BE, EW, FI, IT, and PL, assuming lifelong immunity (MSIR), CW, or AW with cut off $H = 35$ years. The dots represent the observed serological data with size proportional to the population age distribution obtained from demographic data.

Table 2. *ML estimates for the scenario-specific parameters* $q, \boldsymbol{\varepsilon}, \boldsymbol{\sigma}, \varphi$*, and the basic reproduction number* R_0*, with* 95% *bootstrap-based percentile CIs in square brackets, information criteria AIC and BIC (minima indicated in boldface), obtained under the assumption of AW with cut off* $H = 35$ *years*

Country	Model				$\hat{R}_0$		AIC	BIC
BE	MSIRW	$\hat{q}$	0.080	[0.063, 0.096]	3.53	[2.94, 4.30]	3359.11	**3377.19**
		$\hat{\varepsilon}_1$	0.007	[0.005, 0.009]				
		$\hat{\varepsilon}_2$	0.000	[0.000, 0.000]				
	MSIRWb	$\hat{q}$	0.084	[0.065, 0.102]	3.70	[3.05, 4.57]	3361.77	3379.86
		$\hat{\varepsilon}_1$	0.019	[0.012, 0.027]				
		$\hat{\varepsilon}_2$	0.005	[0.001, 0.010]				
	MSIRWb-ext	$\hat{q}$	0.085	[0.067, 0.103]	3.75	[3.08, 4.63]	**3353.63**	3377.74
		$\hat{\varepsilon}_1$	0.013	[0.008, 0.020]				
		$\hat{\varepsilon}_2$	0.000	[0.000, 0.005]				
		$\hat{\varphi}$	0.35	[0.05, 0.94]				
	MSIRS	$\hat{q}$	0.065	[0.056, 0.072]	2.86	[2.61, 3.20]	3359.25	3377.34
		$\hat{\sigma}_1$	0.030	[0.018, 0.049]				
		$\hat{\sigma}_2$	0.010	[0.004, 0.018]				
EW	MSIRW	$\hat{q}$	0.064	[0.054, 0.070]	2.05	[1.84, 2.27]	3521.81	3539.65
		$\hat{\varepsilon}_1$	0.008	[0.004, 0.011]				
		$\hat{\varepsilon}_2$	0.000	[0.000, 0.002]				
	MSIRWb	$\hat{q}$	0.068	[0.056, 0.076]	2.18	[1.92, 2.46]	3514.79	3532.63
		$\hat{\varepsilon}_1$	0.017	[0.008, 0.025]				
		$\hat{\varepsilon}_2$	0.003	[0.000, 0.006]				
	MSIRWb-ext	$\hat{q}$	0.068	[0.057, 0.076]	2.19	[1.93, 2.46]	3514.61	3538.39
		$\hat{\varepsilon}_1$	0.026	[0.010, 0.048]				
		$\hat{\varepsilon}_2$	0.007	[0.000, 0.017]				
		$\hat{\varphi}$	2.03	[0.30, 5.59]				
	MSIRS	$\hat{q}$	0.061	[0.053, 0.065]	1.96	[1.82, 2.10]	**3512.43**	**3530.27**
		$\hat{\sigma}_1$	0.021	[0.010, 0.032]				
		$\hat{\sigma}_2$	0.003	[0.000, 0.007]				
IT	MSIRW	$\hat{q}$	0.029	[0.024, 0.031]	1.96	[1.72, 2.17]	3176.10	3193.59
		$\hat{\varepsilon}_1$	0.006	[0.000, 0.009]				
		$\hat{\varepsilon}_2$	0.001	[0.000, 0.005]				
	MSIRWb	$\hat{q}$	0.029	[0.024, 0.032]	1.99	[1.74, 2.24]	**3174.87**	**3192.36**
		$\hat{\varepsilon}_1$	0.008	[0.000, 0.014]				
		$\hat{\varepsilon}_2$	0.004	[0.000, 0.007]				
	MSIRS	$\hat{q}$	0.028	[0.023, 0.030]	1.90	[1.72, 2.08]	3175.53	3193.02
		$\hat{\sigma}_1$	0.010	[0.000, 0.017]				
		$\hat{\sigma}_2$	0.004	[0.000, 0.008]				

Continued on next page

Table 2. *Continued*

Country	Model				$\hat{R}_0$		AIC	BIC
PL	MSIRW	$\hat{q}$	0.049	[0.041, 0.054]	2.24	[2.00, 2.49]	2788.15	2805.62
		$\hat{\varepsilon}_1$	0.001	[0.000, 0.004]				
		$\hat{\varepsilon}_2$	0.000	[0.000, 0.000]				
	MSIRWb	$\hat{q}$	0.057	[0.044, 0.068]	2.64	[2.11, 3.16]	2770.01	2787.48
		$\hat{\varepsilon}_1$	0.013	[0.001, 0.022]				
		$\hat{\varepsilon}_2$	0.000	[0.000, 0.000]				
	MSIRWb-ext	$\hat{q}$	0.058	[0.047, 0.066]	2.67	[2.29, 3.04]	2752.17	2775.46
		$\hat{\varepsilon}_1$	0.030	[0.018, 0.048]				
		$\hat{\varepsilon}_2$	0.000	[0.000, 0.001]				
		$\hat{\varphi}$	2.45	[1.59, 5.18]				
	MSIRS	$\hat{q}$	0.053	[0.046, 0.056]	2.44	[2.23, 2.60]	**2740.45**	**2757.91**
		$\hat{\sigma}_1$	0.042	[0.014, 0.082]				
		$\hat{\sigma}_2$	0.000	[0.000, 0.001]				

likelihood is rather limited and the curves for the 4 scenarios show distinct optimal values for H, ranging from 5 to 35 years. The tendency toward lower cutoff values for IT and EW seems to be driven by ill-fitting points in infants, which is confirmed through a sensitivity analysis (cf. Section 5). A comparison of the overall likelihood, combined over all countries, for the different values of H and a visual inspection of the fit to the data lead us to the choice of $H = 35$ years.

Table 2 presents the ML estimates and 95% bootstrap-based percentile CIs for the scenario-specific parameters and R_0, assuming a piecewise constant function for ε and σ with a cut off at $H = 35$ years. Figure 2 displays the estimated seroprevalence and force of infection for the age-specific waning (AW) models which overall performed best according to AIC/BIC: MSIRWb-ext and MSIRS. The results for FI are omitted since these are the same as in the CW case (Table 1 and Figure 2). As described for the CW counterpart in Section 4.1, the bootstrap replicates for MSIRWb-ext AW are problematic for IT and therefore the results are not considered here (replaced by MSIRWb AW in Figure 2). The MSIRS AW fit for IT is omitted from Figure 2 since it cannot be differentiated from the MSIRWb AW fit. For BE, EW, and PL, the AW models perform markedly better than their constant counterparts according to AIC and BIC, with the single exception of the MSIRW scenario for PL. The fitted seroprofiles now clearly display a decrease or plateau in young adults (Figure 2). For IT, the AIC values are virtually equal while the CW models have smaller BIC values than the age-specific ones. For BE, EW, and IT, the MSIRW and MSIRS scenarios are quite competitive when it comes to model selection, and it is difficult to discern whether a dynamics involving waning and boosting of immunity or complete loss of immunity potentially leading to multiple infections, is more plausible for PVB19. The Polish results support the latter scenario in which protection acquired through PVB19 infection in childhood may be lost ($\approx$ 24 years after infection), after which secondary infections with PVB19 could occur up till the age of 35 years.

Consistent for all countries and all scenarios, is the finding that the immunity transition rates ε and σ in individuals above 35 years of age are either estimated to be 2 to 7 times smaller than the corresponding rate in younger individuals or that the transition from R to W and S for MSIRW and MSIRS, respectively, even does not occur in individuals of age 35 years and older, which is the case for PL. This may reflect the general observation that infection or boosting through exposure to individuals who are infectious with PVB19, elicits higher antibody responses in mature immune systems, which could prolong the process

Table 3. *ML estimates for the average maternal proportion of susceptibles ($\bar{s}_p$), the average maternal force of infection ($\bar{\lambda}_p$), and the annual number of PVB19 infections (I_p) in pregnant women, the frequency of PVB19 infection in pregnancy (freq), and the annual number of fetal deaths due to PVB19 infection (FD), together with 95% bootstrap-based percentile CIs in square brackets. First entry: CW; second entry (if available): AW with cut off $H = 35$ years*

Country	Model	Waning	$\hat{\bar{s}}_p$		$\hat{\bar{\lambda}}_p$		$\hat{I}_p$		Freq		FD	
BE	MSIR		0.27	[0.23, 0.30]	0.034	[0.028, 0.039]	797	[656, 905]	1 in 143	[126, 174]	31	[25, 35]
	MSIRW	CW	0.17	[0.12, 0.21]	0.046	[0.036, 0.057]	677	[552, 777]	1 in 168	[147, 207]	26	[21, 30]
		AW	0.14	[0.10, 0.17]	0.051	[0.040, 0.062]	622	[509, 721]	1 in 183	[158, 224]	24	[20, 28]
	MSIRWb	CW	0.15	[0.11, 0.19]	0.048	[0.038, 0.060]	652	[526, 760]	1 in 175	[150, 217]	25	[20, 29]
		AW	0.13	[0.09, 0.16]	0.054	[0.042, 0.066]	595	[479, 701]	1 in 192	[163, 238]	23	[18, 27]
	MSIRWb-ext	CW	0.15	[0.11, 0.20]	0.048	[0.038, 0.060]	653	[525, 762]	1 in 175	[150, 217]	25	[20, 29]
		AW	0.12	[0.09, 0.16]	0.054	[0.042, 0.067]	587	[473, 684]	1 in 194	[167, 241]	23	[18, 26]
	MSIRS	CW	0.24	[0.21, 0.27]	0.059	[0.042, 0.082]	1256	[915, 1703]	1 in 91	[67, 125]	48	[35, 66]
		AW	0.29	[0.26, 0.33]	0.077	[0.057, 0.107]	1990	[1431, 2825]	1 in 57	[40, 80]	77	[55, 109]
	MSIRS-ext	CW	0.25	[0.21, 0.27]	0.050	[0.038, 0.145]	1091	[839, 2889]	1 in 105	[39, 136]	42	[32, 111]
EW	MSIR		0.38	[0.35, 0.41]	0.018	[0.015, 0.020]	3373	[2874, 3659]	1 in 192	[177, 226]	130	[111, 141]
	MSIRW	CW	0.32	[0.28, 0.36]	0.021	[0.017, 0.024]	3365	[2867, 3655]	1 in 193	[178, 226]	130	[110, 141]
		AW	0.27	[0.23, 0.32]	0.025	[0.019, 0.028]	3277	[2814, 3580]	1 in 198	[181, 231]	126	[108, 138]
	MSIRWb	CW	0.31	[0.27, 0.36]	0.022	[0.017, 0.025]	3358	[2861, 3649]	1 in 193	[178, 227]	129	[110, 140]
		AW	0.23	[0.19, 0.29]	0.027	[0.020, 0.032]	3181	[2743, 3499]	1 in 204	[186, 237]	122	[106, 135]
	MSIRWb-ext	CW	0.31	[0.27, 0.36]	0.022	[0.017, 0.025]	3354	[2865, 3647]	1 in 194	[178, 227]	129	[110, 140]
		AW	0.23	[0.19, 0.28]	0.028	[0.021, 0.032]	3172	[2741, 3488]	1 in 205	[186, 237]	122	[106, 134]
	MSIRS	CW	0.35	[0.33, 0.38]	0.022	[0.017, 0.026]	3919	[3113, 4469]	1 in 166	[145, 208]	151	[120, 172]
		AW	0.39	[0.36, 0.43]	0.031	[0.023, 0.038]	6156	[4187, 7603]	1 in 105	[85, 155]	237	[161, 293]
	MSIRS-ext	CW	0.36	[0.33, 0.38]	0.022	[0.017, 0.031]	3845	[3140, 5333]	1 in 169	[122, 207]	148	[121, 205]
FI	MSIR		0.43	[0.39, 0.45]	0.014	[0.011, 0.016]	260	[200, 289]	1 in 220	[197, 285]	10	[8, 11]
	MSIRW(b)	CW	0.43	[0.39, 0.45]	0.014	[0.011, 0.016]	260	[200, 290]	1 in 220	[197, 285]	10	[8, 11]
	MSIRS	CW	0.43	[0.39, 0.45]	0.014	[0.011, 0.016]	260	[201, 294]	1 in 220	[194, 284]	10	[8, 11]

Continued on next page

Table 3. *Continued*

Country	Model	Waning	$\hat{s}_p$		$\hat{\lambda}_p$	$\hat{I}_p$		Freq	FD	
IT	MSIR		0.38	[0.36, 0.41]	0.010	[0.007, 0.011]	1590	[1277, 1764]	1 in 354	[319, 440]	61	[49, 68]
	MSIRW	CW	0.32	[0.28, 0.37]	0.012	[0.009, 0.014]	1594	[1282, 1782]	1 in 353	[316, 439]	61	[49, 69]
		AW	0.29	[0.25, 0.36]	0.013	[0.009, 0.014]	1583	[1278, 1778]	1 in 355	[316, 440]	61	[49, 68]
	MSIRWb	CW	0.31	[0.27, 0.37]	0.012	[0.009, 0.014]	1591	[1282, 1781]	1 in 354	[316, 439]	61	[49, 69]
		AW	0.28	[0.24, 0.36]	0.013	[0.009, 0.015]	1577	[1269, 1776]	1 in 357	[317, 443]	61	[49, 68]
	MSIRS	CW	0.36	[0.34, 0.39]	0.013	[0.009, 0.015]	1957	[1452, 2294]	1 in 288	[245, 387]	75	[56, 88]
		AW	0.38	[0.34, 0.42]	0.014	[0.010, 0.018]	2356	[1509, 3019]	1 in 238	[186, 373]	91	[58, 116]
	MSIRS-ext	CW	0.36	[0.34, 0.39]	0.012	[0.009, 0.015]	1888	[1443, 2387]	1 in 298	[236, 390]	73	[56, 92]
PL	MSIR		0.31	[0.28, 0.33]	0.024	[0.019, 0.028]	2208	[1753, 2577]	1 in 173	[148, 218]	85	[67, 99]
	MSIRW(b)	CW	0.31	[0.28, 0.33]	0.024	[0.019, 0.028]	2208	[1753, 2569]	1 in 173	[149, 218]	85	[67, 99]
	MSIRW	AW	0.29	[0.25, 0.32]	0.025	[0.019, 0.030]	2147	[1726, 2469]	1 in 178	[155, 221]	83	[66, 95]
	MSIRWb	AW	0.21	[0.16, 0.29]	0.030	[0.021, 0.037]	1854	[1470, 2225]	1 in 206	[172, 260]	71	[57, 86]
	MSIRWb-ext	AW	0.21	[0.17, 0.26]	0.030	[0.023, 0.036]	1832	[1477, 2192]	1 in 208	[174, 259]	71	[57, 84]
	MSIRS	CW	0.31	[0.28, 0.33]	0.024	[0.019, 0.028]	2208	[1753, 2586]	1 in 173	[148, 218]	85	[67, 100]
		AW	0.38	[0.32, 0.42]	0.065	[0.036, 0.100]	7277	[3386, 12305]	1 in 52	[31, 113]	280	[130, 474]

of antibody waning. Further, we obtain the following $\hat{R}_0$ ranges for the AW scenarios: 2.86–3.75 for BE, 1.96–2.19 for EW, 1.90–2.02 for IT, and 2.24–2.67 for PL, which are significantly larger than the basic reproduction number for FI (Table 1).

4.3 *Risk in pregnancy*

For each of the scenarios considered for each country in the 2 previous sections, Table 3 presents the ML estimates for $\bar{s}_p$, $\bar{\lambda}_p$, and I_p, the frequency of PVB19 infection in pregnancy, and the annual number of fetal deaths due to PVB19 infection, with corresponding 95% bootstrap-based percentile CIs. Our results for the MSIR model can be compared to the results of Mossong, Hens, Friederichs, *and others* (2008) who analyzed the same serological surveys using local quadratic models based on the assumption of lifelong immunity. With the social contact data approach, we find similar estimates for the average maternal proportion of susceptibles $\bar{s}_p$ to PVB19: 27%, 38%, 43%, 38%, and 31%, for BE, EW, FI, IT, and PL, respectively. The largest difference is found for PL for which Mossong, Hens, Friederichs, *and others* (2008) obtained an estimate of 37%. It should be noted that our MSIR scenario does not provide a good fit to the Polish serology since it is not flexible enough to capture the decrease in young adults. The maternal risk $\bar{\lambda}_p$ of acquiring PVB19 infection when still susceptible is estimated to be 0.034 (BE), 0.018 (EW), 0.014 (FI), 0.010 (IT), and 0.024 (PL), which in case of BE is significantly larger than the estimate of 0.006 obtained by Mossong, Hens, Friederichs, *and others* (2008). Also, for EW and PL, we estimate a larger maternal force of infection and in summary for BE and EW, we estimate a significantly higher frequency of PVB19 infection in pregnancy compared to Mossong, Hens, Friederichs, *and others* (2008) and Vyse *and others* (2007).

For the MSIRW scenarios presented in Table 3, we notice either no change or a slight decrease in the estimated frequency of PVB19 infection in pregnancy and the induced number of fetal deaths, when broadly comparing them to the MSIR model. In contrast for the MSIRS scenarios, the estimated frequency is much higher for BE, EW, IT, and PL (AW) with a significant difference observed for the former and latter country. These 2 trends continue when comparing the CW models to their AW counterparts: for the MSIRW scenarios, allowing for AW induces a decrease in the estimated frequency of PVB19 infection in pregnancy, while it induces an increase for the MSIRS scenarios. The annual number of fetal deaths due to PVB19 infection in pregnancy, estimated from MSIR, MSIRWb AW, and MSIRS AW, respectively, equals 31, 23, and 77 for BE, 130, 122, and 237 for EW, 10 for FI, 61, 61, and 91 for IT, and 85, 71, and 280 for PL. Our estimates for the average maternal force of infection for PVB19 are in line with the seroconversion rates reported in literature, which are estimated from prospective cohort studies in pregnant women (Valeur-Jensen *and others*, 1999; Alanen *and others*, 2005; van Gessel *and others*, 2006).

4.4 *Age-dependent proportionality of the transmission rates*

As noted in Section 3.2, we assess the sensitivity of the results from our model structure analysis for PVB19 with respect to the constant proportionality assumption of the transmission rates. Here, we highlight the main results, but for a detailed description, we refer to Appendix D.1 of the Supplementary Material available at *Biostatistics* online. For the CW case, by allowing q to be age-dependent, the evidence of waning immunity found for BE, EW, and IT, is almost completely absorbed, while for FI and PL, the results from Section 4.1 remain practically unaltered. For the AW models for BE, EW, and PL, however, the evidence in favor of waning immunity is sustained under the age-dependent proportionality assumption, and the scenario-specific parameter estimates are fairly close to what was obtained before.

5. Discussion

The results in Sections 4.1 and 4.2 for BE, EW, and PL, indicate substantial evidence toward processes of AW immunity for PVB19. Furthermore, this finding is preserved when we relax the constant proportionality assumption of the transmission rates (Section 4.4). Figure 2 demonstrates that the AW scenarios are able to explain the observed decrease in the seroprofile for adults. The waning rates $\boldsymbol{\varepsilon}$ and $\boldsymbol{\sigma}$ are consistently estimated to be smaller in individuals above 35 years of age, which may reflect a stronger antibody response in more mature immune systems when exposed to PVB19, prolonging the subsequent waning process of IgG antibodies. It is however difficult to discern from the data whether a scenario involving waning and boosting of low immunity or a scenario allowing for reinfections, is more plausible for PVB19. This is also illustrated by a small simulation study presented in Appendix E of the Supplementary Material available at *Biostatistics* online. Elucidating the underlying immunological process for PVB19 is nevertheless important with respect to maternal-fetal risk assessment as we have shown in Section 4.3 in which the MSIRS scenarios predict a higher risk of PVB19 infection in pregnancy and a larger associated number of fetal deaths.

For IT, the evidence against lifelong immunity for PVB19 is merely sustained under the assumption of constant proportionality and is less pronounced than for BE, EW, and PL. From the Finnish serological data, we cannot infer any evidence of waning immunity for PVB19, which relates to the shape of the seroprofile. The Finnish seroprofile plateaus between the ages of 20 and 40 years and does not display a decrease as for the other countries. For both FI and IT, we obtain smaller estimates for the basic reproduction number R_0, and it could be hypothesized that the reduced potential of spread for PVB19 in these countries makes it more difficult to observe long-term waning processes at the population level. There is a limit to what can be inferred from serological surveys, and we believe we have reached the boundary of what is estimable by considering models such as MSIRWb-ext, MSIRS-ext, and MSIRWS. In Appendix F of the Supplementary Material available at *Biostatistics* online, we provide, in addition to the results here, estimates for the average number of transitions from one stage to the other per person during their lifetime and the average age at which these transitions occur.

In our model structure analysis, we have assumed endemic equilibrium for PVB19 which means that disease incidence fluctuates around a stationary average over time. The few reports in the literature suggest that PVB19 has 3–5 year epidemic cycles in European countries with a seasonal peak in the first half of each year (Bosman *and others*, 2002; Riipinen *and others*, 2008; Vyse *and others*, 2007), comparable to rubella. Using auxiliary data on case reports, Whitaker and Farrington (2004) show that cyclic epidemics have only a marginal effect on estimates obtained under endemic equilibrium from serological surveys for immunizing infections with short latent and infectious periods. Whether these findings can be extended toward nonimmunizing infections has not been investigated yet and is beyond the scope of this paper.

It was noted that the serological data reveal a rather high proportion of seropositive 1-year old infants (Mossong, Hens, Friederichs, *and others*, 2008), which decreases until the second or third year of life and then starts to increase gradually, except for IT where a similar pattern is detected from 3 years of age. One would however expect that the proportion of seropositive infants immediately starts to build up after the loss of maternal antibodies. Mossong, Hens, Friederichs, *and others* (2008) suggest that this could be due to a lack of assay specificity for these age groups exposed to many other viral agents. On the other hand, cyclic PVB19 epidemics in relation to the timing of the data collections could perhaps also explain these observations. The proportion of seropositive neonates born in the period after an epidemic will be lower than expected, whereas the number of congenital infections during an epidemic, and thus the proportion of seropositive newborns will be larger. Yet, we are not able to verify this hypothesis due to lack of data on the epidemic patterns for the countries involved in this study.

Given these seropositivity "deviations" in infants, we performed a sensitivity analysis by omitting the serological samples for infants aged 0.5–3 years and refitting all models. The same scenarios and cutoff

points for the AW models are selected according to AIC and BIC, except for EW and IT where in case of the MSIRW scenarios the cutoff point is not anymore selected at young ages. Overall, the ML estimates of the model parameters, R_0 and the risk in pregnancy are approximately the same. Only for the MSIRS scenario in EW, IT, and PL, we observe a slight decrease in $\hat{q}$ and $\hat{\boldsymbol{\sigma}}$, inducing smaller estimates for the number of fetal deaths.

There is a need for additional large prospective cohort studies in pregnant women in order to obtain more precise estimates of the risk of fetal death and hydrops fetalis due to PVB19 infection. In Miller *and others* (1998) and Enders *and others* (2004), only pregnant women who were reported because they had rash, arthropathy, or other symptoms, and/or contact with a suspected case of erythema infectiosum, were included in the analysis (at the point when maternal PVB19 infection was serologically confirmed). This selection, with a reduced probability of asymptomatic PVB19 cases to be reported, may compromise the generalization of the estimated risk to the entire population of pregnant women.

SUPPLEMENTARY MATERIAL

Supplementary material is available at http://biostatistics.oxfordjournals.org.

ACKNOWLEDGMENTS

We are grateful to Jacco Wallinga and Mirjam Kretzschmar for providing valuable comments during the DIMACS/ECDC workshop "Spatio-temporal and Network Modelling of Diseases III" in Tübingen, 2008. This work benefited from discussions held with John Edmunds from the London School of Hygiene & Tropical Medicine, and Pierre Van Damme, Heidi Theeten, Elke Leuridan, and Tessa Braeckman from the Centre for the Evaluation of Vaccination at the University of Antwerp. *Conflict of Interest:* None declared.

FUNDING

"SIMID," a strategic basic research project funded by the Institute for the Promotion of Innovation by Science and Technology in Flanders (IWT) (060081); We also gratefully acknowledge support from the IAP research network nr P6/03 of the Belgian Government (Belgian Science Policy).

REFERENCES

ALANEN, A., KAHALA, K., VAHLBERG, T., KOSKELA, P. AND VAINIONPÄÄ, R. (2005). Seroprevalence, incidence of prenatal infections and reliability of maternal history of varicella zoster virus, cytomegalovirus, herpes simplex virus and parvovirus B19 infection in South-Western Finland. *BJOG: An International Journal of Obstetrics and Gynaecology* **112**, 50–56.

ANDERSON, M. AND CHERRY, J. (2004). *Textbook of Pediatric Infectious Diseases*, Chapter 17. Philadelphia, PA: Saunders, pp. 1796.

ANDERSON, R. AND MAY, R. (1991). *Infectious Diseases of Humans: Dynamics and Control*. Oxford: Oxford University Press.

BOSMAN, A., WALLINGA, J. AND KROES, A. (2002). Elke vier jaar de vijfde ziekte: parvovirus B19. *Infectieziekten Bull.* **6**, 215–219.

COHEN, B. (1995). Parvovirus B19: an expanding spectrum of disease. *British Medical Journal* **311**, 1549–1552.

DIEKMANN, O., HEESTERBEEK, J. AND METZ, J. (1990). On the definition and the computation of the basic reproduction ratio R_0 in models for infectious diseases in heterogeneous populations. *Journal of Mathematical Biology* **28**, 365–382.

EDMUNDS, W., O'CALLAGHAN, C. AND NOKES, D. (1997). Who mixes with whom? A method to determine the contact patterns of adults that may lead to the spread of airborne infections. *Proceedings of the Royal Society of London, Series B: Biological Sciences* **264**, 949–957.

ENDERS, G., MILLER, E., CRADOCK-WATSON, J., BOLLEY, I. AND RIDEHALGH, M. (1994). Consequences of varicella and herpes zoster in pregnancy: prospective study of 1739 cases. *Lancet* **343**, 1548–1551.

ENDERS, M., WEIDNER, A., ZOELLNER, I., SEARLE, K. AND ENDERS, G. (2004). Fetal morbidity and mortality after acute human parvovirus B19 infection in pregnancy: prospective evaluation of 1018 cases. *Prenatal Diagnosis* **24**, 513–518.

GAY, N. (1996). Analysis of serological surveys using mixture models: application to a survey of parvovirus B19. *Statistics in Medicine* **15**, 1567–1573.

GAY, N., HESKETH, L., COHAN, B., RUSH, B. C., MORGAN-CAPNER, P. AND MILLER, E. (1994). Age specific antibody prevalence to parvovirus B19: how many women are infected in pregnancy? *Communicable Disease Report* **4**, R104–R107.

GOEYVAERTS, N., HENS, N., OGUNJIMI, B., AERTS, M., SHKEDY, Z., VAN DAMME, P. AND BEUTELS, P. (2010). Estimating infectious disease parameters from data on social contacts and serological status. *Applied Statistics* **59**, 255–277.

HEEGAARD, E. AND BROWN, K. (2002). Human parvovirus B19. *Clinical Microbiology Reviews* **15**, 485–505.

HUATUCO, E., DURIGON, E., LEBRUN, F., PASSOS, S., GAZETA, R., AZEVEDO NETO, R. AND MASSAD, E. (2008). Seroprevalence of human parvovirus B19 in a suburban population in Sao Paulo, Brazil. *Revista de Saúde Pública* **42**, 443–449.

KAUFMANN, J., BUCCOLA, J., STEAD, W., ROWLEY, C., WONG, M. AND BATES, C. (2007). Secondary symptomatic parvovirus B19 infection in a healthy adult. *Journal of General Internal Medicine* **22**, 877–878.

MILLER, E., FAIRLEY, C., COHEN, B. AND SENG, C. (1998). Immediate and long term outcome of human parvovirus B19 infection in pregnancy. *British Journal of Obstetrics and Gynaecology* **105**, 174–178.

MOSSONG, J., HENS, N., FRIEDERICHS, V., DAVIDKIN, I., BROMAN, M., LITWINSKA, B., SIENNICKA, J., TRZCINSKA, A., VAN DAMME, P., BEUTELS, P. *and others* (2008). Parvovirus B19 infection in five European countries: seroepidemiology, force of infection and maternal risk of infection. *Epidemiology and Infection* **136**, 1059–1068.

MOSSONG, J., HENS, N., JIT, M., BEUTELS, P., AURANEN, K., MIKOLAJCZYK, R., MASSARI, M., SALMASO, S., SCALIA-TOMBA, G., WALLINGA, J. *and others* (2008). Social contacts and mixing patterns relevant to the spread of infectious diseases. *PLoS Medicine* **5**, 381–391.

NASCIMENTO, J., BUCKLEY, M., BROWN, K. AND COHEN, B. (1990). The prevalence of antibody to human parvovirus B19 in Rio De Janeiro, Brazil. *Revista do Instituto de Medicina Tropical de Sao Paulo* **32**, 41–45.

PASTUSZAK, A., LEVY, M., SCHICK, B., ZUBER, C., FELDKAMP, M., GLADSTONE, J., BAR-LEVY, F., JACKSON, E., DONNENFELD, A., MESCHINO, W. *and others* (1994). Outcome after maternal varicella infection in the first 20 weeks of pregnancy. *The New England Journal of Medicine* **330**, 901–905.

RIIPINEN, A., VÄISÄNEN, E., NUUTILA, M., SALLMEN, M., KARIKOSKI, R., LINDBOHM, M.-L., HEDMAN, K., TASKINEN, H. AND SÖDERLUND-VENERMO, M. (2008). Parvovirus B19 infection in fetal deaths. *Clinical Infectious Diseases* **47**, 1519–1525.

ROUDERFER, V., BECKER, N. AND HETHCOTE, H. (1994). Waning immunity and its effects on vaccination schedules. *Mathematical Biosciences* **124**, 59–82.

SCHNEIDER, B., HÖNE, A., TOLBA, R., FISCHER, H., BLÜMEL, J. AND EIS-HÜBINGER, A. (2008). Simultaneous persistence of multiple genome variants of human parvovirus B19. *Journal of General Virology* **89**, 164–176.

SCHOUB, B., BLACKBURN, N., JOHNSON, S. AND MCANERNEY, J. (1993). Primary and secondary infection with human parvovirus B19 in pregnant women in South Africa. *South African Medical Journal* **83**, 505–506.

SELF, S. AND LIANG, K.-Y. (1987). Asymptotic properties of maximum likelihood estimators and likelihood ratio tests under nonstandard conditions. *Journal of the American Statistical Association* **82**, 605–610.

TOLFVENSTAM, T., PAPADOGIANNAKIS, N., NORBECK, O., PETERSSON, K. AND BROLIDEN, K. (2001). Frequency of human parvovirus B19 in intrauterine fetal death. *Lancet* **357**, 1494–1497.

VALEUR-JENSEN, A. K., PEDERSEN, C. B., WESTERGAARD, T., JENSEN, I. P., LEBECH, M., ANDERSEN, P. K., AABY, P., PEDERSEN, B. N. AND MELBYE, M. (1999). Risk factors for parvovirus B19 infection in pregnancy. *Journal of the American Medical Association* **281**, 1099–1105.

VAN BOVEN, M., DE MELKER, H., SCHELLEKENS, J. AND KRETZSCHMAR, M. (2000). Waning immunity and sub-clinical infection in an epidemic model: implications for pertussis in The Netherlands. *Mathematical Biosciences* **164**, 161–182.

VAN BOVEN, M., DE MELKER, H., SCHELLEKENS, J. AND KRETZSCHMAR, M. (2001). A model based evaluation of the 1996-7 pertussis epidemic in The Netherlands. *Epidemiology and Infection* **127**, 73–85.

VAN GESSEL, P., GAYTANT, M., VOSSEN, A., GALAMA, J., URSEM, N., STEEGERS, E. AND WILDSCHUT, H. (2006). Incidence of parvovirus B19 infection among an unselected population of pregnant women in The Netherlands: a prospective study. *European Journal of Obstetrics, Gynecology and Reproductive Biology* **128**, 46–49.

VYSE, A., ANDREWS, N., HESKETH, L. AND PEBODY, R. (2007). The burden of parvovirus B19 infection in women of childbearing age in England and Wales. *Epidemiology and Infection* **135**, 1354–1362.

WALLINGA, J., TEUNIS, P. AND KRETZSCHMAR, M. (2006). Using data on social contacts to estimate age-specific transmission parameters for respiratory-spread infectious agents. *American Journal of Epidemiology* **164**, 936–944.

WHITAKER, H. AND FARRINGTON, C. (2004). Estimation of infectious disease parameters from serological survey data: the impact of regular epidemics. *Statistics in Medicine* **23**, 2429–2443.

YOUNG, N. AND BROWN, K. (2004). Parvovirus B19. *The New England Journal of Medicine* **350**, 586–597.

[*Received May 28, 2010; revised August 11, 2010; accepted for publication August 13, 2010*]